European Journal of Radiology 187 (2025) 112129

Contents lists available at ScienceDirect

European Journal of Radiology

journal homepage: www.elsevier.com/locate/ejrad

Research article

Non-contrast dual-energy CT iodine quantification for lung injury characterization after balloon pulmonary angioplasty

Alfredo Páez-Carpio [a,b,c,d,*], Llúria Cornellas [e], Blanca Domenech-Ximenos [b], Elena Serrano [f], Joan A. Barberà [c,d,g,h], Fernando M. Gómez [i], Isabel Blanco [c,d,g,h,1], Ivan Vollmer [e,1]

[a] Department of Medical Imaging, University of Toronto, Toronto M5T1W7 ON, Canada
[b] Department of Radiology, CDI, Hospital Clínic Barcelona, Barcelona 08036, Spain
[c] Institut d'Investigacions Biomèdiques August Pi i Sunyer (IDIBAPS), Barcelona 08036, Spain
[d] Faculty of Medicine and Health Sciences, Universitat de Barcelona, Barcelona 08036, Spain
[e] Department of Radiology, Hospital Universitari Vall d'Hebron, Barcelona 08035, Spain
[f] Department of Radiology, Hospital Universitari de Bellvitge, L'Hospitalet de Llobregat 08907, Spain
[g] Biomedical Research Networking Centre on Respiratory Diseases (CIBERES), Madrid, Spain
[h] Department of Pulmonary Medicine, ICR, Hospital Clínic Barcelona, Barcelona 08036, Spain
[i] Department of Radiology, Hospital Universitari i Politècnic La Fe, València 46026, Spain

ARTICLE INFO

Keywords:
Balloon angioplasty
Dual-energy
Computed tomography
Pulmonary hypertension
Pulmonary thromboembolism

ABSTRACT

*Objectives*This study aimed to identify differences in iodine concentrations in new-onset pulmonary injuries and normal lung parenchyma after balloon pulmonary angioplasty (BPA) for chronic thromboembolic pulmonary hypertension (CTEPH) using non-contrast dual-energy CT (NC-DECT) between patients with pulmonary hemorrhage and reperfusion pulmonary edema.

Methods: Patients undergoing NC-DECT after BPA between January 2019 and April 2023 due to hemoptysis or clinical worsening were retrospectively evaluated for inclusion. Patients were divided based on the presence or absence of BPA-related hemoptysis. Intralesional iodine concentrations were measured in new-onset lung injuries, adjacent normal parenchyma, same lobe, and contralateral lung. CT morphological features, including lesion shape, imaging pattern, absolute density, and ROI size, were recorded. Statistical comparisons were performed using Mann-Whitney U, Friedman, and Wilcoxon signed-rank tests.

Results: Thirteen patients with 32 new-onset post-BPA lung injuries were included. Median iodine concentration in lung injuries was significantly higher in patients with hemoptysis than those without (3.4 mg/mL versus 0.6 mg/mL; $p < 0.001$). In the hemoptysis group, iodine concentration in lung injuries was significantly higher compared with the different locations of normal lung parenchyma ($p < 0.001$). In the non-hemoptysis group, no significant differences in iodine concentration were observed between lung injuries and normal parenchyma ($p = 0.167$; $p = 0.351$; $p = 0.246$). Absolute density ($p = 0.767$), lesion shape ($p = 0.610$), imaging appearance ($p = 0.530$), ROI area ($p = 0.452$), and halo sign ($p = 0.810$) showed no significant correlation with hemoptysis.

Conclusion: NC-DECT identifies iodine concentration differences in lung injuries between patients with and without hemoptysis after BPA. Elevated iodine concentrations may serve as an imaging marker for post-procedural pulmonary hemorrhage.

Critical relevance statement: This exploratory study demonstrates the potential of NC-DECT in distinguishing between pulmonary hemorrhage and reperfusion pulmonary edema in lung injuries after BPA in patients with CTEPH. The ability to quantify iodine concentrations in lung lesions offers a novel imaging biomarker for pulmonary hemorrhage, which could play a pivotal role in improving clinical decision-making and management strategies for patients undergoing BPA.

Abbreviations: **BPA**, Balloon pulmonary angioplasty; **CTEPH**, Chronic thromboembolic pulmonary hypertension; **DECT**, Dual-energy CT; **GGO**, ground-glass opacity; **HU**, Hounsfield units; **ICM**, Iodinated contrast media; **NC-DECT**, Non-contrast dual-energy CT; **PEA**, Pulmonary endarterectomy; **ROI**, region-of-interest.

* Corresponding author at: 263 McCaul St 4th floor, Toronto, ON M5T 1W7, Canada.
E-mail address: alfredo.paezcarpio@mail.utoronto.ca (A. Páez-Carpio).

[1] These authors collaborated equally as co-senior authors.

https://doi.org/10.1016/j.ejrad.2025.112129
Received 16 February 2025; Received in revised form 26 March 2025; Accepted 20 April 2025
Available online 21 April 2025

1. Introduction

Balloon pulmonary angioplasty (BPA) is the invasive alternative treatment (class I recommendation by the European Society of Cardiology/European Respiratory Society) for patients with chronic thromboembolic pulmonary hypertension (CTEPH) not amenable to pulmonary endarterectomy (PEA) [1–4]. Postprocedural lung injury represents one of the most prevalent complications associated with BPA, with rates between 4–10 % [5,6]. The causal mechanism underlying post-BPA lung injury remains elusive. Initial reports hypothesized that it resulted from reperfusion pulmonary edema, akin to lung injury observed after PEA [7,8]. Nevertheless, it has been suggested that most of these new-onset lung injuries may be attributed to pulmonary hemorrhage due to vascular injury [9,10].

Hemoptysis is the only available clinical marker for pulmonary hemorrhage [9]. Using conventional imaging techniques, distinguishing these two separate causes of lung injury in the absence of hemoptysis is difficult. Efforts have been made to determine radiological signs that differentiate them, such as consolidation in the parenchyma around the treated vessel. However, these signs are generally interchangeable in both conditions [11]. Therefore, additional imaging biomarkers beyond conventional radiological signs could help to improve diagnostic accuracy and guide clinical management. Proper differentiation characterization of subclinical pulmonary hemorrhage may have significant clinical implications. Pulmonary hemorrhage necessitates close clinical monitoring, antibiotics, corticosteroids, and potential reversal of any anticoagulation therapy the patient may be receiving. In contrast, reperfusion pulmonary edema treatment is generally treated with oxygen supplementation and diuretics [12].

Dual-energy CT (DECT) allows the reconstruction of iodine-specific images, enabling various applications such as lesion detection and characterization in oncology, the characterization of cerebral hemorrhage after mechanical thrombectomy and several applications in the lung [13–20]. Notably, Takeuchi et al. demonstrated that DECT enables differentiation between cardiogenic pulmonary edema and acute interstitial lung disease. Their findings indicated that cardiogenic pulmonary edema does not exhibit elevated intralesional iodine levels compared to normal lung parenchyma, as opposed to acute interstitial lung disease [21]. Reperfusion pulmonary edema results from increased water in the extravascular space due to a rapid rise in pulmonary perfusion after vascular recanalization, while pulmonary hemorrhage is caused by vascular injury and blood extravasation into the lung parenchyma [19,22]. Following this principle, we propose that non-contrast DECT (NC-DECT) could distinguish these conditions by quantifying the iodine extravasated during the BPA procedure in pulmonary hemorrhage, in contrast to the absence of iodine elevation in edema, as demonstrated by Takeuchi et al. [21]. NC-DECT was chosen to eliminate the confounding effect of systemic contrast, ensuring that measured iodine reflects extravasation from vascular injury rather than circulating contrast.

Therefore, this study was designed to compare iodine concentration measurements obtained using NC-DECT in new-onset lung injuries following BPA, aiming to determine whether this imaging technique can accurately differentiate between pulmonary hemorrhage and reperfusion pulmonary edema using post-procedural hemoptysis as the clinical marker for pulmonary hemorrhage.

2. Material and methods

2.1. Study design

This study was approved by our institution's institutional review board and adhered to the STROBE Statement and the Declaration of Helsinki. Informed consent was obtained from all participants. A retrospective, single-center, single-arm study was designed to evaluate the ability of NC-DECT to quantify extravasated iodinated contrast medium (ICM) in lung injuries caused by BPA in patients with CTEPH and, therefore, differentiate pulmonary hemorrhage from reperfusion pulmonary edema. To achieve this, the study assessed differences in iodine concentration between new-onset lung injuries in patients with hemoptysis and compared with intralesional iodine concentrations of patients without hemoptysis, as hemoptysis is the clinical marker for pulmonary hemorrhage. These measurements were also compared with those in normal lung parenchyma of the same patient. Patients were consecutively recruited between January 2019 and April 2023 as they underwent NC-DECT following BPA (Fig. 1). Data were retrospectively gathered from electronic medical records using a dedicated, study-specific anonymized database.

2.2. Patient selection

Patients aged 18 years or older with diagnosed CTPEH and treated with BPA and undergoing a post-procedural NC-DECT evaluation were consecutively evaluated for inclusion. Patients underwent NC-DECT mainly in two situations: intra- or *peri*-procedural hemoptysis or deterioration of respiratory symptoms with new-onset lung injury on routine post-procedural chest X-ray. Deterioration of respiratory symptoms was primarily characterized by increased dyspnea compared to the pre-BPA baseline, often accompanied by decreased oxygen saturation, chest discomfort, or fatigue with reduced exercise tolerance. Exclusion criteria included lack of pre-procedural CT, incorrect protocol during NC-DECT acquisition, inability to retrieve images, and poor imaging quality. All patients undergoing BPA at our institution are systematically evaluated to exclude significant pre-existing pulmonary conditions, including malignancies, through comprehensive imaging, physical examination, and laboratory workup prior to each procedure.

2.3. BPA procedure and post-procedure management

All BPA procedures were performed in a monoplane angio-suite (*ARTIS-Q, Siemens Healthineers*®) by two experienced interventional radiologists with 3–10 years of experience. Patients routinely stayed one day in the intermediate care unit and one day in the conventional ward. At least one post-procedural imaging test, typically a chest X-ray, was performed. A NC-DECT was performed in cases of hemoptysis or worsening of respiratory symptoms and the presence of a new-onset lung injury on chest X-rays. IMC used was Omnipaque 300, administered as required for the procedure, with a dilution of 80:20 (ICM:normal saline).

2.4. NC-DECT protocol

NC-DECT was performed using a *Siemens Healthineers SOMATOM Definition Flash*®. Patients were positioned supine on the CT scan. For the DECT settings, the kV parameters were set at a low energy of 80–90 kV for Tube A and a high energy of 140–150 kV for Tube B. The mA settings were adjusted using the Care Dose optimization system, typically between 100 and 300 mAs. A preliminary scanogram was conducted to confirm accurate scan range and patient positioning, extending from the pulmonary apex to the celiac trunk. No delayed scan time was used. Pitch was set to 0.6, with an exposure time per rotation of 0.25 s. Collimation was established at 0.6 mm, with a slice thickness of 0.6 mm. The field of view was tailored to the widest part of the thorax, using a reconstruction matrix of 512. Iterative reconstruction was used using the *Siemens Healthineers ADMIRE*® software at a moderate strength level (Level 3). Imaging was performed without the administration of ICM. Diagnostic reconstruction filters were set to Br40 for mediastinal evaluation and Br64 for lung evaluation. Axial reconstructions were conducted with a slice thickness of 1 mm for mediastinal, 1 mm for lung series and 1 mm for DECT diagnostic series used for iodine concentration measurement (Table 1).

2.5. Data collection and NC-DECT Reading

Two board-certified radiologists participated in data collection and image analysis. A radiologist with three years of experience reviewed clinical and procedural data, including patient demographics, baseline hemodynamic parameters, BPA indications, procedural details, and post-procedural complications such as hemoptysis. Data were extracted from electronic medical records and compiled into a dedicated anonymized database.

A second board-certified radiologist with 20 years of experience in chest imaging, blinded to all clinical data, independently analyzed all NC-DECT scans. New-onset BPA-related lung injuries were defined as ground-glass opacities (GGO) or consolidations appearing within 24 h after BPA in the treated lung parenchyma. Iodine concentrations were measured using circular regions of interest (ROIs) manually drawn to include at least 80 % of the lesion while avoiding vessels, bronchi, and artifacts (Fig. 2). Measurements were also obtained from adjacent normal lung parenchyma, the same lobe, and the contralateral lung for comparison (Fig. 3). Iodine quantification was performed using the Siemens Healthineers Syngo.Via® software, with periodic software updates applied throughout the study period.

Classical CT morphological features of lung injuries were documented, including lesion shape (triangular, rounded, or ovoid), imaging pattern (GGO, consolidation, or mixed), absolute density in Hounsfield units (HU), lesion extent (graded 1 to 5), and the presence of the halo sign. The total ROI area was recorded in cm^2. These imaging characteristics were analyzed to assess their correlation with iodine concentration and hemoptysis status.

2.6. Outcomes

The primary outcome was the difference in intralesional iodine concentrations in new-onset lung injuries between patients with intra or post-procedural pulmonary hemorrhage and those without *peri*-procedural pulmonary hemorrhage. Patients were clinically classified as having pulmonary hemorrhage or no pulmonary hemorrhage based on the presence of peri- or post-procedural hemoptysis. The secondary outcome evaluated the difference in iodine concentration between post-procedural lung injuries and different locations of normal parenchyma in the same patient and the difference between iodine concentrations in normal parenchyma between hemoptysis and no hemoptysis patients. The relationship between the different morphological characteristics on CT, intralesional iodine concentration, and the presence of hemoptysis was also evaluated.

Table 1
Non-contrast dual-energy CT protocol.

Protocol	Post- BPA NC-DECT
Patient position	Supine
Extension	From pulmonary apex to celiac trunk
ICM	No
Scanogram	Yes
Dual-energy kV	Tube A: 80–90 kV Tube B: 140–150 kV
mA	CareDose: 100–300 mA
Delayed scan time	No
Pitch	0.6
Exposure time	0.25 s per rotation
Collimation	0.6 mm
Slice thickness adquisition	0.6 mm
Reconstruction matrix	512
Iterative reconstruction	*Yes*, moderate strentght level
Reconstruction filters	Br40 for mediastinal evaluation Br64 for pulmonary evaluation
Slice thickness for diagnosis	1 mm

NC-DECT: non-contrast dual-energy CT. kV: kilovolt. mA: milliamps. mSv: millisievert. ICM: iodinated contrast médium.

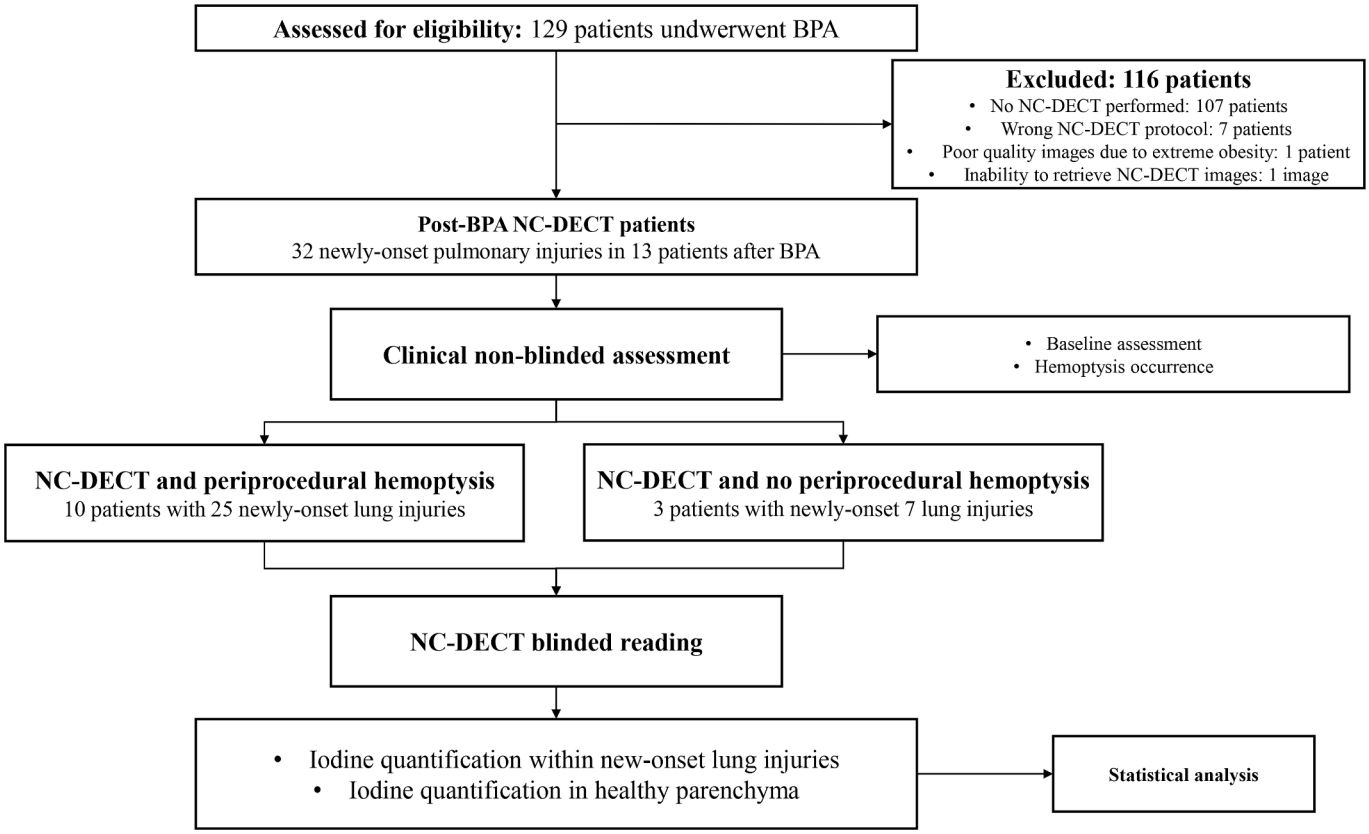

Fig. 1. Study design.

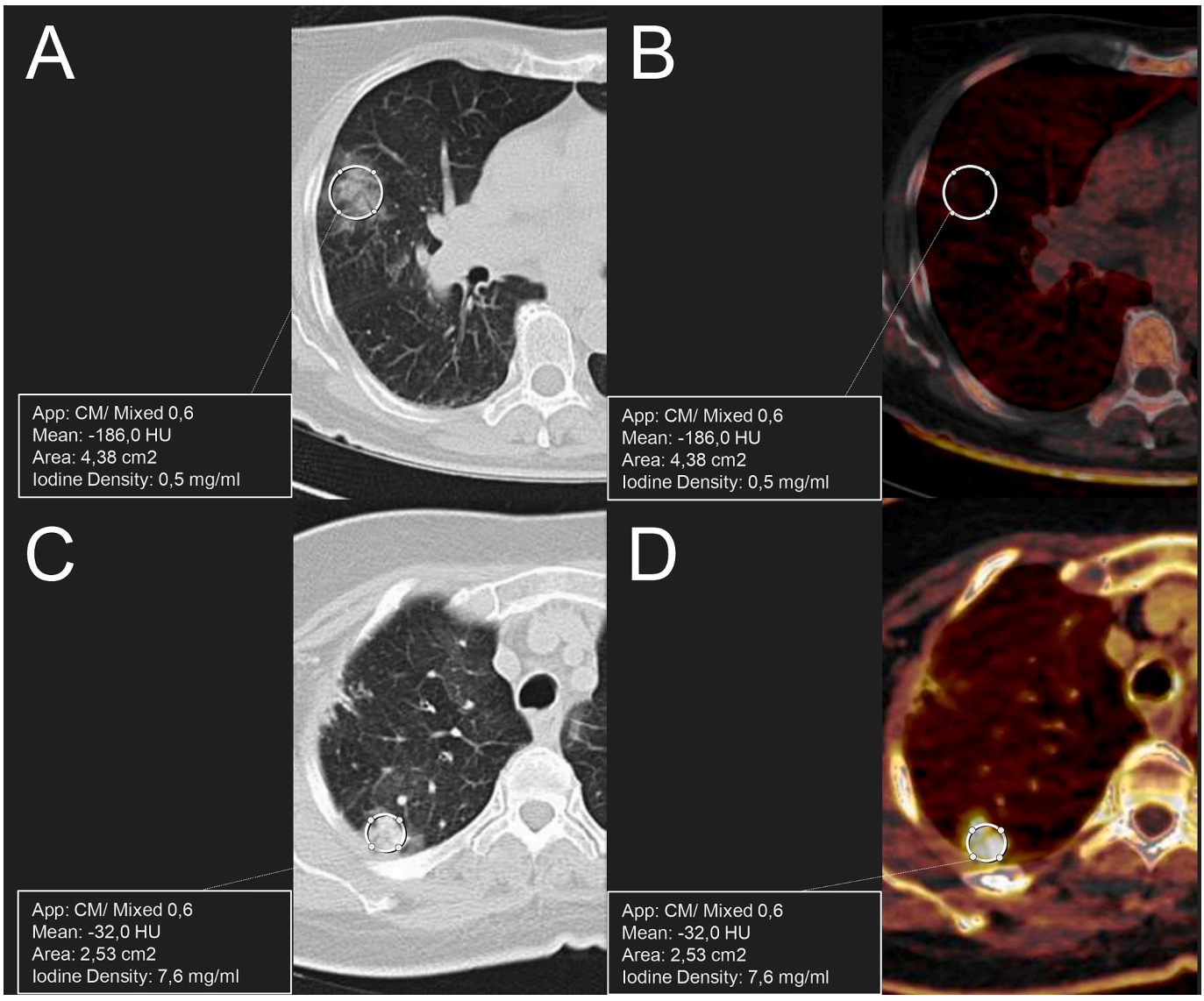

Fig. 2. Examples of lung injuries with normal and elevated iodine levels. Examples of post-BPA lung injuries with normal and elevated intralesional iodine levels. (**A-B**) Non-contrast dual-energy CT scan of a new-onset pulmonary injury with normal iodine levels in a 52-year-old female patient presenting with worsening dyspnea after BPA. (**A**) Axial lung window image shows a new-onset ground-glass lung injury in the lateral segment of the middle lobe. A circular ROI encompassing at least 80 % of the lesion is demonstrated. (**B**) Axial iodine map image at the same level as (**A**) reveals no enhancement within the new-onset lung injury in the middle lobe. Intralesional iodine concentration is low (0.5 mg/mL). (**C-D**) Non-contrast dual-energy CT scan of a new-onset lung lesion with elevated iodine levels in a 68-year-old male patient experiencing intraprocedural hemoptysis. (**C**) Axial lung window image demonstrates a new-onset lung injury with mixed ground-glass and consolidation components in the apical segment of the right upper lobe. A circular ROI encompassing at least 80 % of the lesion is displayed. (**D**) Axial iodine map image at the same level as (**C**) shows qualitative and quantitative elevations in intralesional iodine concentration compared to the surrounding normal parenchyma, with a measured value of 7.6 mg/mL.

2.7. Data analysis

Descriptive statistics were performed using the mean and standard deviation for quantitative variables or the median and interquartile range if the variable did not follow a normal distribution. Qualitative variables were characterized using absolute and relative frequencies of each category. Friedman test was used for within-subject comparisons, including comparing iodine concentrations across different lung locations within the same subjects. Following significant Friedman test results, post-hoc analyses were conducted using Wilcoxon signed-rank tests for pairwise comparisons between locations. Mann-Whitney U tests were used for between-group comparisons, e.g., comparing iodine concentrations between patients with or without hemoptysis. Spearman correlation analyses were performed to evaluate the relationship between absolute density and iodine concentration and the temporal stability of iodine concentrations following BPA. Kruskal-Wallis tests were used to compare iodine concentrations across different imaging appearance categories and between intra- and *peri*-procedural hemoptysis groups. Chi-square tests were conducted to assess associations between qualitative variables, such as imaging morphology and the occurrence of hemoptysis. All statistical tests were two-tailed, with a significance level set at $p < 0.05$. All statistical analyses were performed using IBM SPSS Statistics (v29.0.2.0).

3. Results

3.1. Baseline characteristics

Between January 2019 and April 2023, 129 BPA sessions were performed in our institution. Of these, 22 patients underwent a post-

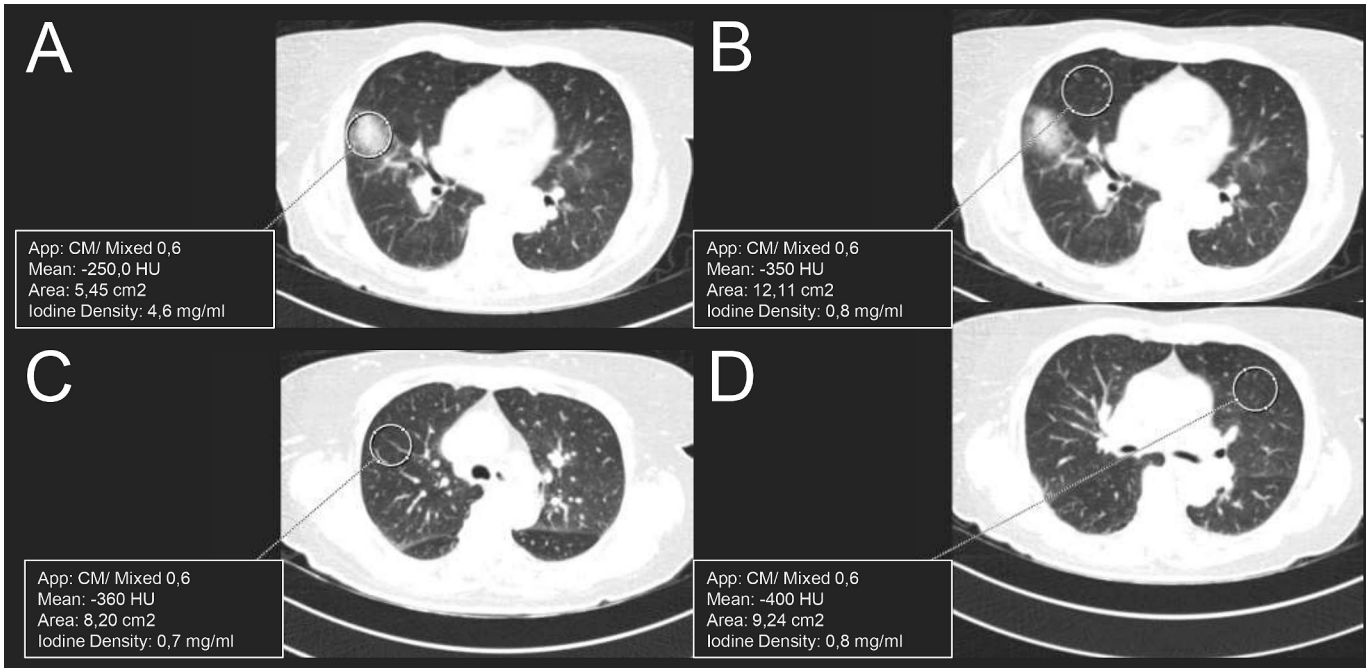

Fig. 3. Iodine measurements within the lung injury and in normal parenchyma. (A-D) Non-contrast dual-energy CT in a 66-year-old male patient who had just undergone BPA and presented hemoptysis. (**A**) Measurement of iodine concentration within the lung injury (*red circle*). (**B**) Measurement of iodine concentration in the normal lung parenchyma immediately adjacent to the lung injury (*red circle*). (**C**) Measurement of iodine concentration in normal lung parenchyma in the same lobe of the lung injury (*red circle*). (**D**) Measurement of iodine concentration in normal lung parenchyma in the lung contralateral to the lung injury (*red circle*).

procedural NC-DECT. Nine patients were excluded; the most common reason was using a wrong protocol during CT acquisition (n = 7, 77.8 %). Thus, 13 patients with 32 new-onset lung injuries after BPA were included in the final analysis. Median age was 64 years (IQR: 48–73) and 7 were female (53.8 %). The most common indication for BPA was the presence of lesions not amenable to surgery (n = 12, 92.3 %). Most patients had clinically and hemodynamically severe CTEPH, with the majority having a New York Heart Association functional classification of III-IV (n = 9, 62.2 %), a median of 40 mmHg (25–47) for mean pulmonary arterial pressure, and a median pulmonary vascular resistance of 7.1 Wood units (2.9–7.5).

3.2. Procedure and post-procedure characteristics

Overall median total amount of ICM used per procedure was 225 mL (IQR: 192.6–257.4), with 227 mL (IQR: 196–270) in the hemoptysis group and 245 mL (IQR: 194–280) in the no hemoptysis group. Median time between BPA procedure completion and NC-DECT acquisition was 50 min (IQR: 44–55). NC-DECT was indicated for intra or periprocedural hemoptysis after BPA in 10 patients (76.9 %). Three patients (23.1 %) were indicated NC-DECT after worsening of clinical parameters and the presence of new-onset lung injury in the post-procedural chest X-ray. Patients with BPA-related hemoptysis presented 25 (78.1 %) new-onset lung injuries and patients with no hemoptysis presented the remaining 7 (23.9 %). Overall median number of lung injuries per patient was 2 (IQR: 1–4), with a median number in patients with hemoptysis of 2 (IQR: 1–4) and 1 in patients with no hemoptysis (IQR: 1–5). All baseline characteristics are shown in Table 2.

3.3. CT morphological characteristics results

Overall median absolute density of all new-onset lung injuries after BPA was −201 HU (IQR: [-286]–[-113]). Overall median ROI area was 4.1 cm^2 (IQR: 2.1–8.4). The halo sign was present in 8 lung injuries (25 %). Most post-BPA lung injuries were round (20, 62.5 %) and exhibited a combined ground-glass and consolidative imaging pattern (24, 75 %).

Table 2
Baseline patient characteristics.

	Overall	Hemoptysis	No Hemoptysis
	n = 13	n = 10	n = 3
Age, *years*	64 (48–73)	68 (21.3–32.1)	50 (45–50)
BMI, *kg/m²*	26.2 (21.3–31.6)	27 (21.3–32.3)	21.3 (14.1–21.3)
Gender, *female*	6 (54.2)	5 (50)	2 (66.7)
BPA indication			
Not amenable to surgery	12 (92.3)	9 (90)	3 (100)
Residual PH after PEA	1 (7.7)	1 (10)	0 (0)
NYHA-FC			
I-II	4 (30.8)	2 (20)	2 (66.7)
III-IV	9 (69.2)	8 (80)	1 (33.3)
6MWD, *meters*	410 (336–424)	390 (334–420)	480 (410–480)
mPAP, *mmHg*	40 (25–47)	41.5 (26–47)	23 (15–23)
PVR, *WU*	7.1 (2.9–7.5)	7.2 (3.5–7.7)	2.9 (1.8–2.9)
Total ICM per procedure	235 (197–270)	227 (196–270)	245 (194–280)
Time until NC-DECT, *minutes*	50 (44–55)	50 (43–55)	46 (46–50)
Lung injuries per patient	2 (1–4)	2 (1–4)	1 (1–5)
Symptoms other than hemoptysis			
Lung injury with no hemoptysis	3 (23.1)	0 (0)	3 (100)
Dyspnea/tachypnea	10 (76.9)	7 (70)	3 (100)
Vasovagal syncope	1 (7.7)	0 (0)	1 (33.3)
Desaturation	7 (53.9)	5 (50)	2 (66.6)

Categorical variables are expressed in **total values (%)** and continuous variables in **median (interquartile range)**.
6MWD: 6 min walking distance. BMI: body mass index. BPA: balloon pulmonary angioplasty. ICM: iodinated contrast medium. mPAP: mean pulmonary artery pressure. NYHA-FC: New York Heart Association functional class. PEA: pulmonary endarterectomy. PVR: peripheral vascular resistance.

No statistically significant differences were observed in these characteristics between patients with hemoptysis and those without hemoptysis ($p = 0.767$, $p = 0.452$, $p = 0.810$, $p = 0.610$ and $p = 0.530$, respectively) (Table 3).

3.4. Iodine quantification measurement results

Overall median iodine concentration in all new-onset lung injuries after BPA was 2.9 mg/mL (IQR: 1.1–4.2). Median iodine concentration of lung injuries in patients with documented intra or periprocedural hemoptysis was **3.4 mg/mL (IQR: 2.0–4.7)** and lung injury median iodine concentration for patients without hemoptysis was **0.6 mg/mL (IQR: 0.3–1.0)**, with statistically significant differences between measurements of the two groups (**$p < 0.001$**) (Fig. 4). No significant differences were found in normal parenchymal iodine concentrations measurements between the two groups (Table 4).

Statistically significant differences were also detected between the iodine concentration within new-onset lung injuries compared to all three normal lung parenchyma locations in patients diagnosed with *peri*-procedural hemoptysis (**$p < 0.001$**). No significant differences were observed between iodine concentrations of new-onset lung injuries in patients with no *peri*-procedural hemoptysis and measurements in normal parenchyma in those same patients (**$p = 0.167$; $p = 0.351$; $p = 0.246$**) (Fig. 5).

Iodine intralesional concentration in lung injuries was moderately associated with absolute density ($p = 0.043$), with higher iodine levels correlating with increased HU values. No significant differences in iodine concentration were observed based on lesion shape ($p = 0.960$), the presence of a halo sign ($p = 0.16$), or the timing of hemoptysis (intra- vs. *peri*-procedural, $p = 0.26$). However, iodine concentrations were significantly higher in consolidations compared to ground-glass opacities ($p = 0.021$) and mixed patterns ($p = 0.004$). Additionally, no relationship was observed between intralesional iodine concentration and the time between the completion of the procedure and NC-DECT acquisition ($p = 0.330$) or between the occurrence of intra- or *peri*-procedural hemoptysis ($p = 0.267$).

4. Discussion

This study demonstrates the feasibility of using NC-DECT to differentiate new-onset lung injuries following BPA, distinguishing those caused by pulmonary hemorrhage from those resulting from reperfusion pulmonary edema by using intralesional iodine concentrations as an imaging biomarker. Lung injuries following BPA in patients with hemoptysis—clinical marker of pulmonary hemorrhage—showed higher intralesional iodine concentrations compared to lung injuries in patients without hemoptysis. Furthermore, in patients with hemoptysis, iodine concentration measurements in new-onset lung injuries were higher compared to normal lung parenchyma, whereas, in patients without hemoptysis, concentrations of pathological and normal lung parenchyma were similar. In contrast, classical CT features such as absolute density, lesion shape, imaging appearance, ROI area and the presence of a halo sign showed no significant differences between patients with and without hemoptysis, demonstrating the limitations of these traditional imaging parameters in differentiating the underlying etiology of post-BPA lung injuries.

To our knowledge, this is the first study exploring the use of NC-DECT in characterizing new-onset lung injury following BPA in patients with CTEPH. Takeuchi et al. previously examined the potential of DECT in differentiating cardiogenic pulmonary edema from acute interstitial lung disease edema by comparing iodine concentration measurements in patients clinically diagnosed with either condition [21]. Their findings indicated no significant difference in iodine concentration between affected and normal lung parenchyma in patients with cardiogenic pulmonary edema. In contrast, patients with acute interstitial lung disease exhibited a significantly higher iodine concentration in the affected lung parenchyma, with values two-fold greater than those observed in normal parenchyma [21]. Our study partially adopted its methodology from this exploratory study. However, given that the patient sample in our study shared the same underlying pathology and underwent the same procedure, we opted to compare the iodine concentrations in post-BPA new-onset lung injuries in patients with clinically confirmed pulmonary hemorrhage evidenced by hemoptysis and those without hemoptysis, as well as with the healthy parenchyma of each patient. Our findings confirm the observation by Takeuchi et al. that pulmonary edema tends to show iodine concentrations similar to those of healthy lung parenchyma, while also validating our hypothesis that extravasated iodine secondary to vascular injury in post-BPA pulmonary hemorrhage can be detected using NC-DECT. Interestingly, our study identified a finding not reported by Takeuchi et al.: the correlation between absolute density in HU, the type of lung lesion—specifically pulmonary consolidation—and intralesional iodine concentration. This observation is theoretically consistent, as higher iodine concentrations are expected to contribute to increased lesion density. However, this correlation did not extend to a significant relationship with hemoptysis. Specifically, no significant differences in HU values or imaging appearance of lung injuries were observed between patients with and without hemoptysis, nor across different lesion appearances. In contrast, a clear association was observed between elevated iodine concentrations and the presence of hemoptysis. This discrepancy may be explained by the fact that HU measurements reflect a combination of factors—such as tissue density, air content, and iodine concentration—whereas iodine quantification provides a more precise and reliable measurement that is unaffected by these confounding variables.

Several studies have attempted to characterize new-onset post-BPA lung injury using conventional CT. Early studies aimed to characterize new-onset pulmonary injury following BPA presumed to be the equivalent of reperfusion pulmonary edema reported after PEA [23]. In the initial study on BPA for CTEPH, Feinstein et al. reported an incidence of post-BPA lung injury of 61 %, all attributed to reperfusion pulmonary edema. More recent studies with a more refined BPA technique reported incidences of lung injuries in the range of 20–30 %, also attributed to reperfusion pulmonary edema [7,24]. However, other teams have proposed that PEA and BPA are distinct procedures, suggesting that the pathophysiological mechanism underlying most post-BPA lung injuries may differ from reperfusion pulmonary edema observed following PEA. Ejiri et al. sought to illustrate this by characterizing post-BPA lung injuries using conventional CT in all patients who underwent BPA,

Table 3
CT classical characteristics of new-onset lung injuries and their relationship with hemoptysis and iodine concentration.

	Overall	Hemoptysis	No Hemoptysis	*p-value*
	n = 32	n = 25	n = 7	
Density, *HU*	−201 ([-286]–[-113])	−199 ([-315]–[-99])	−204 ([-245]–[-186])	*p* = 0.77
ROI area, *cm²*	4.1 (2.1–8.4)	4.1 (2.3–9.9)	4 (1.2–8.1)	*p* = 0.45
Halo sign, *yes*	8 (25 %)	6 (24)	2 (28.6)	*p* = 0.81
Morphology				*p* =
Round	20 (62.5)	16 (64)	4 (57.1)	0.61
Triangular	2 (6.3)	2 (8)	0 (0)	
Ovoid	10 (31.3)	7 (28)	3 (42.9)	
Imaging pattern				*p* = 0.53
Ground-glass	4 (12.5)	3 (12)	1 (14.3)	
Consolidative	4 (12.5)	4 (16)	0 (0)	
Mixed	24 (75)	18 (72)	6 (85.7)	

Categorical variables are expressed in **total values (%)** and continuous variables in **median (interquartile range)**.
HU: Hounsfield units. ROI: region of interest. cm^2: centimeters squared.

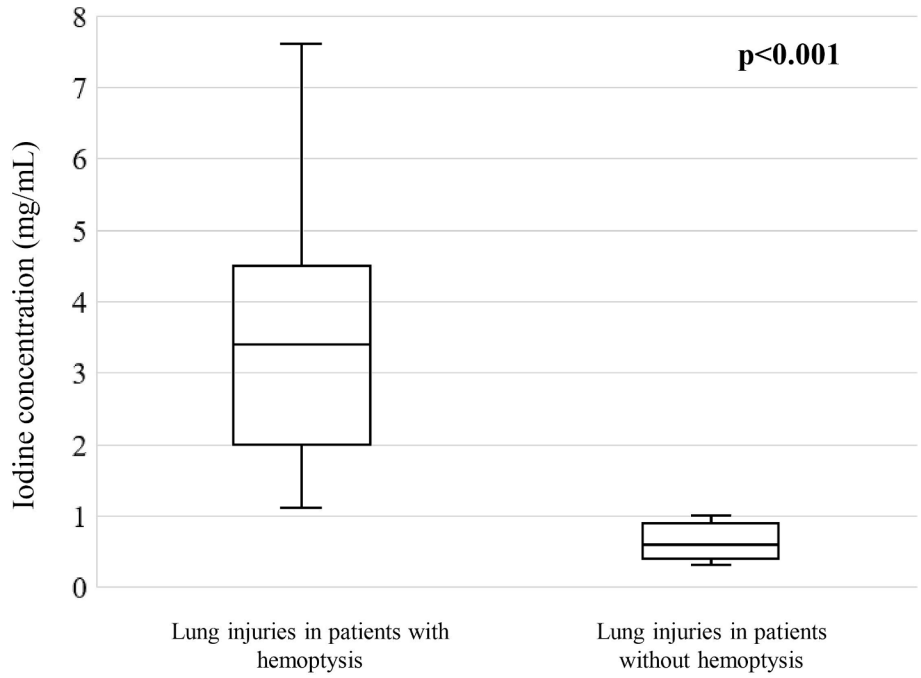

Fig. 4. Box-and-whisker plots showing iodine concentration in new-onset lung injuries in all patients included in the study. Mean iodine concentration is significantly higher in lung injuries in patients with BPA-related hemoptysis compared with patients without hemoptysis ($p < 0.001$).

Table 4
Iodine quantitation results and statistical analysis comparing results of patients with periprocedural hemoptysis and patients without hemoptysis.

Iodine quantification results	Overall	Hemoptysis	No Hemoptysis	*p-value*
	n = 32	n = 25	n = 7	
Newly-onset lung injuries, *mg/mL*	2.9 (1.1–4.2)	3.4 (2.0–4.7)	0.6 (0.3–1.0)	***p < 0.001***
Normal lung parenchyma, *mg/mL*				
Immediately adjacent to lung injury	0.8 (0.4–1.1)	0.8 (0.4–1.2)	0.6 (0.1–0.8)	*p = 0.351*
Same lobe as lung injury	0.8 (0.5–1.0)	0.8 (0.6–1.2)	0.8 (0.4–1.1)	*p = 0.611*
Contralateral lung to lung injury	0.8 (0.5–1.0)	0.6 (0.5–1.2)	0.5 (0.3–0.7)	*p = 0.246*

Categorical variables are expressed in **total values (%)** and continuous variables in **median (interquartile range)**.
Mann-Whitney *U* test was used for between-group comparisons.
Bold p-values represent statistically significant results ($p < 0.05$).

including asymptomatic cases [9]. They suggest that, given the imaging characteristics of most injuries observed in their study, these may correspond to pulmonary hemorrhage rather than reperfusion pulmonary edema [9]. However, in our opinion, making this assertion based solely on conventional CT is challenging. Both pathologies closely resemble each other, typically presenting as focal GGO or consolidations. To further investigate this issue, we conducted an analysis evaluating the correlation between various classical CT features, including absolute density, ROI area, lesion shape, imaging appearance (ground-glass opacity, consolidation, and mixed patterns), and the presence of a halo sign, with the occurrence of hemoptysis. The analysis revealed no significant correlations, further supporting the conclusion that classical imaging features alone are insufficient for accurately characterizing post-BPA lung lesions. Our study demonstrates that intralesional iodine concentration measurements can serve as an imaging biomarker for characterizing post-BPA lung injuries, providing a complementary tool beyond the mere description of lesion morphology. Thus, our findings indicate that NC-DECT iodine quantification may offer complementary information to conventional imaging features, which alone appear insufficient for distinguishing pulmonary hemorrhage from reperfusion pulmonary edema.

In routine clinical practice, measuring iodine concentrations in new-onset lung injuries as an imaging biomarker to distinguish between reperfusion pulmonary edema and pulmonary hemorrhage could significantly impact post-procedural management for patients undergoing BPA for CTEPH. Accurate characterization of post-BPA lung injuries is essential, as, in cases of pulmonary hemorrhage, delaying the resumption of chronic oral anticoagulation could help reduce the incidence of subacute post-procedural hemoptysis [25–28]. Conversely, for cases of reperfusion pulmonary edema, the immediate start of diuretic therapy could reduce the length of hospital stay [20]. Early interventions, such as the use of non-invasive positive pressure ventilation, have also shown to improve hypoxemia and potentially prevent mechanical ventilation in patients with reperfusion pulmonary edema after pulmonary angioplasty [27]. Therefore, incorporating intralesional iodine quantification into routine post-BPA evaluations may enhance the characterization of in-situ lung injuries, facilitating more personalized and timely interventions for these patients.

This study is limited by its retrospective, single-center design, small sample size, and inclusion of only patients with post-BPA complications, introducing selection bias and limiting the assessment of asymptomatic cases. The short median time between BPA and NC-DECT may have restricted the evaluation of post-procedural changes, and the higher pre-test probability of pulmonary hemorrhage in patients with hemoptysis affects the generalizability of findings. While hemoptysis was used as a clinical marker for pulmonary hemorrhage, some cases may occur without it, and vascular injury can be present with or without hemoptysis, as noted in the 2023 BPA consensus, suggesting the need to validate iodine quantification against broader vascular injury criteria. Additionally, circular ROIs instead of free-hand ROIs may have introduced quantification bias, and potential confounders such as procedural variations and comorbidities were not accounted for. Future studies could also explore regional variations of iodine concentration within individual lung lesions to enhance lesion characterization and assess temporal changes in iodine distribution over longer follow-up periods.

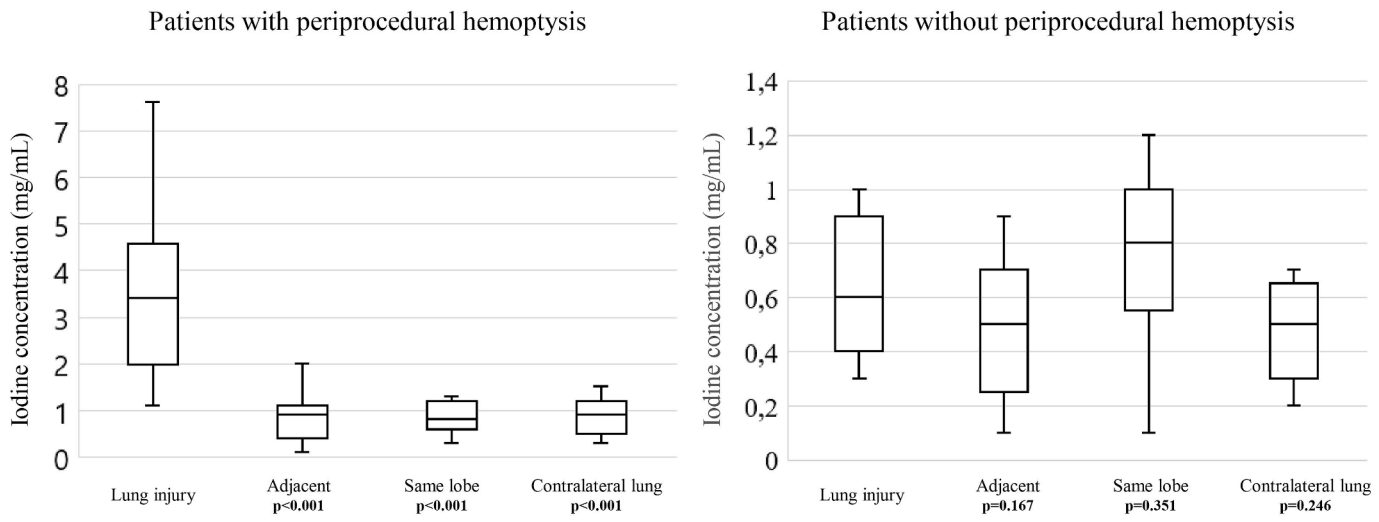

Fig. 5. Box-and-whisker plots showing iodine concentration in the normal and affected areas of all patients in the study. Median iodine concentration significantly higher in lung injuries in patients with BPA-related hemoptysis compared with different locations of normal lung parenchyma ($p < 0.001$). Comparatively, mean iodine concentration is comparable between the normal lung parenchyma and lung injuries in patients without hemoptysis and affected areas ($p = 0.167$; $p = 0.351$; $p = 0.246$).

Also, although iodine elevation likely reflects contrast extravasation, inflammatory microvascular leakage cannot be excluded, highlighting the need for histopathological validation. Future prospective studies should refine the role of NC-DECT in differentiating pulmonary hemorrhage from reperfusion edema and expand its application to asymptomatic cases.

5. Conclusion

NC-DECT intralesional iodine quantification is an effective method for differentiating pulmonary hemorrhage from reperfusion pulmonary edema in post-BPA patients. These findings suggest NC-DECT could serve as a non-invasive biomarker to guide clinical decision-making and improve post-procedural management in patients undergoing BPA for CTEPH. However, further prospective studies with larger, more diverse populations are required to validate these results and assess the broader applicability of NC-DECT in post-BPA management.

6. Declarations

6.2. Availability of data and material

The dataset used for this study is not publicly available as institutional consent for data sharing was not obtained from Hospital Clínic Barcelona. However, data may be made available by the corresponding author upon reasonable request and subject to institutional approval.

CRediT authorship contribution statement

APC: Writing – review & editing, Writing – original draft, Visualization, Validation, Supervision, Software, Resources, Project administration, Methodology, Investigation, Formal analysis, Data curation, Conceptualization. **LC:** Writing – review & editing, Visualization, Validation. **BDX:** Writing – review & editing, Visualization, Validation. **ES:** Writing – review & editing, Writing – original draft, Validation. **JAB:** Writing – review & editing, Writing – original draft, Validation. **FMG:** Writing – review & editing, Writing – original draft, Validation, Supervision. **IB:** Writing – review & editing, Validation, Supervision. **IV:** Writing – review & editing, Visualization, Validation, Supervision, Project administration, Methodology, Investigation, Formal analysis, Data curation, Conceptualization.

6.1. Ethics approval and consent to participate

This retrospective study was waived from informed consent by the Committee on Drug Research Ethics (CEIm) of Hospital Clínic Barcelona (HCB/2023/0591). We carried out the study in accordance with the Declaration of Helsinki.

Funding

This research did not receive any specific grant from funding agencies in the public, commercial, or not-for-profit sectors.

Declaration of competing interest

The authors declare that they have no known competing financial interests or personal relationships that could have appeared to influence the work reported in this paper.

Acknowledgements

In loving memory of Alejandro Páez-Carpio, MD.

XpertScientific Editing and Consulting Services provided editorial assistance, including language editing and correction and consulting regarding statistical analysis.

References

[1] M. Humbert, G. Kovacs, M.M. Hoeper, et al., The 2022 ESC/ERS Guidelines for the diagnosis and treatment of pulmonary hypertension, Eur. Respir. J. 61 (2023) 2200879, https://doi.org/10.1183/13993003.00879-2022.

[2] M.M. Hoeper, Pharmacological therapy for patients with chronic thromboembolic pulmonary hypertension, Eur. Respir. Rev. 24 (2015) 272–282, https://doi.org/10.1183/16000617.00002215.

[3] P. Escribano-Subias, I. Blanco, M. López-Meseguer, et al., Survival in pulmonary hypertension in Spain: insights from the Spanish registry, Eur. Respir. J. 40 (2012) 596–603, https://doi.org/10.1183/09031936.00126011.

[4] J. Pepke-Zaba, M. Delcroix, I. Lang, et al., Chronic thromboembolic pulmonary hypertension (CTEPH): results from an international prospective registry, Circulation 124 (2011) 1973–1981, https://doi.org/10.1161/CIRCULATIONAHA.110.015008.

[5] K. Hirakawa, E. Yamamoto, S. Takashio, et al., Balloon pulmonary angioplasty in chronic thromboembolic pulmonary hypertension, Cardiovasc. Interv. Ther. 37 (2022) 60–65, https://doi.org/10.1007/s12928-021-00775-x.

[6] J.M. Moriarty, S.N. Khan, S.D. Kao, et al., Balloon pulmonary angioplasty for chronic thromboembolic pulmonary hypertension, Cardiovasc. Intervent. Radiol. 41 (2018) 1826–1839, https://doi.org/10.1007/s00270-018-1994-7.

[7] H. Mizoguchi, A. Ogawa, M. Munemasa, et al., Refined Balloon Pulmonary Angioplasty for Inoperable Patients with Chronic Thromboembolic Pulmonary Hypertension. 5 (2012) 748–755, https://doi.org/10.1161/CIRCINTERVENTIONS.112.971077.
[8] M. Kataoka, T. Inami, K. Hayashida, et al., Percutaneous transluminal pulmonary angioplasty for the treatment of chronic thromboembolic pulmonary hypertension, Circ. Cardiovasc. Interv. 5 (2012) 756–762, https://doi.org/10.1161/CIRCINTERVENTIONS.112.970749.
[9] K. Ejiri, A. Ogawa, S. Fujii, et al., Vascular injury is a major cause of lung injury after balloon pulmonary angioplasty in patients with chronic thromboembolic pulmonary hypertension, Circ. Cardiovasc. Interv. 11 (2018), https://doi.org/10.1161/CIRCINTERVENTIONS.117.005884.
[10] N. Jain, M.A. Sheikh, D. Bajaj, et al., Periprocedural complications with balloon pulmonary angioplasty, JACC Cardiovasc. Interv. 16 (2023) 976–983, https://doi.org/10.1016/j.jcin.2023.02.019.
[11] A. Páez-Carpio, I. Vollmer, F.X. Zarco, et al., Imaging of chronic thromboembolic pulmonary hypertension before, during, and after balloon pulmonary angioplasty, Diagn. Interv, Imaging 105 (2024) 215–226, https://doi.org/10.1016/j.diii.2023.10.006.
[12] G. Loosen, D. Taboada, E. Ortmann, et al., How would I treat my own chronic thromboembolic pulmonary hypertension in the perioperative period? J. Cardiothorac. Vasc. Anesth. 38 (2024) 884–894, https://doi.org/10.1053/j.jvca.2023.07.028.
[13] S. Lennartz, J. Cao, N. Pisuchpen, et al., Intra-patient variability of iodine quantification across different dual-energy CT platforms: assessment of normalization techniques, Eur. Radiol. (2024), https://doi.org/10.1007/s00330-023-10560-z.
[14] Y. Nagayama, T. Inoue, S. Oda, et al., Adrenal adenomas versus metastases: diagnostic performance of dual-energy spectral CT virtual noncontrast imaging and iodine maps, Radiology 296 (2020) 324–332, https://doi.org/10.1148/radiol.2020191833.
[15] J. Marcon, A. Graser, D. Horst, et al., Papillary vs clear cell renal cell carcinoma: differentiation and grading by iodine concentration using DECT–correlation with microvascular density, Eur. Radiol. 30 (2020) 1–10, https://doi.org/10.1007/s00330-019-06377-3.
[16] K. Hellbach, A. Sterzik, W. Sommer, et al., Dual-energy CT allows for improved characterization of response to antiangiogenic treatment in patients with metastatic renal cell cancer, Eur. Radiol. 27 (2017) 2532–2537, https://doi.org/10.1007/s00330-016-4613-7.
[17] M. Meyer, P. Hohenberger, D. Overhoff, et al., Dual-energy CT vital iodine tumor burden for response assessment in patients with metastatic GIST undergoing TKI therapy, AJR Am. J. Roentgenol. 218 (2022) 659–667, https://doi.org/10.2214/AJR.21.25936.
[18] H. Takeuchi, S. Suzuki, H. Machida, et al., Can dual-energy computed tomography help distinguish cardiogenic pulmonary edema and acute interstitial lung disease? J. Comput. Assist. Tomogr. 42 (2018) 39–44, https://doi.org/10.1097/RCT.0000000000000677.
[19] I.M. Lang, A.K. Andreassen, A. Andersen, et al., Balloon pulmonary angioplasty for chronic thromboembolic pulmonary hypertension: a clinical consensus statement, Eur. Heart J. 44 (2023) 2659–2671, https://doi.org/10.1093/eurheartj/ehad217.
[20] R. Ito, J. Yamashita, S. Ikeda, et al., Predictors of procedural complications in balloon pulmonary angioplasty for chronic thromboembolic pulmonary hypertension, J. Cardiol. 82 (2023) 497–503, https://doi.org/10.1016/j.jjcc.2023.01.010.
[21] H. Takeuchi, S. Suzuki, H. Machida, et al., Preliminary results: can dual-energy computed tomography help distinguish cardiogenic pulmonary edema and acute interstitial lung disease? J. Comput. Assist. Tomogr. 42 (2018) 39–44, https://doi.org/10.1097/RCT.0000000000000677.
[22] T. Inami, M. Kataoka, N. Shimura, et al., Pulmonary edema predictive scoring index (PEPSI), a new index to predict risk of reperfusion pulmonary edema in percutaneous transluminal pulmonary angioplasty, JACC Cardiovasc. Interv. 6 (2013) 725–736, https://doi.org/10.1016/j.jcin.2013.03.009.
[23] A. Adams, P.F. Fedullo, Postoperative management of the patient undergoing pulmonary endarterectomy, Semin. Thorac. Cardiovasc. Surg. 18 (2006) 250–256, https://doi.org/10.1053/j.semtcvs.2006.10.003.
[24] R. Bashir, A. Noory, E. Oliveros, et al., Refined balloon pulmonary angioplasty in chronic thromboembolic pulmonary hypertension, JACC Adv. 2 (2023) 100291, https://doi.org/10.1016/j.jacadv.2023.100291.
[25] N. Ikeda, S. Kubota, T. Okazaki, et al., The predictors of complications in balloon pulmonary angioplasty for chronic thromboembolic pulmonary hypertension, Catheter. Cardiovasc. Interv. 93 (2019) E349–E356, https://doi.org/10.1002/ccd.28133.
[26] I. Lang, B.C. Meyer, T. Ogo, et al., Balloon pulmonary angioplasty in chronic thromboembolic pulmonary hypertension, Eur. Respir. Rev. 26 (2017) 160119, https://doi.org/10.1183/16000617.0119-2016.
[27] S. Minatsuki, A. Kiyosue, A. Saito, et al., Effectiveness of nitroglycerin in managing subacute lung bleeding induced by balloon pulmonary angioplasty, Int. Heart J. 59 (2018) 899–901, https://doi.org/10.1536/ihj.17-566.
[28] K. Hosokawa, T. Yamamoto, K. Abe, et al., Delayed-onset lung injury after balloon pulmonary angioplasty for chronic thromboembolic pulmonary hypertension—a case report, Eur. Heart J. Cardiovasc. Imaging 18 (2017) 1426, https://doi.org/10.1093/ehjci/jex116.